Hindawi
Advances in Civil Engineering
Volume 2018, Article ID 5678253, 10 pages
https://doi.org/10.1155/2018/5678253

Research Article

Vibration and Dynamic Response of Buffering Devices during the Vertical Feeding of Coal Mine Solid Backfill Materials

Feng Ju, Zequan He, Meng Xiao, Peng Huang, and Shuai Guo

State Key Laboratory for Geomechanics and Deep Underground Engineering, China University of Mining and Technology, Xuzhou 221116, China

Correspondence should be addressed to Feng Ju; juf1983@163.com

Received 23 April 2018; Revised 29 August 2018; Accepted 25 November 2018; Published 13 December 2018

Guest Editor: Fengqiang Gong

The stability of buffering devices is very important for the continuous vertical feeding of solid backfill materials. Based on the characteristics of the vertical feeding system, the functional characteristics of buffering devices were analyzed and a buffering device was designed in this paper. The finite element models for the buffering device were established by using the ANSYS software, and the dynamic response and mode characteristics of these models were studied. The results show that the distribution of the equivalent stress on the buffering device surface is petal shaped, in which the stress reaches the maximum at the center and gradually decrease to all around. The stress of support beams is highest at both ends and lowest at the center. Besides, the resonant frequency of this buffering device is 2.4 Hz, which means this frequency should be avoided during the process of backfill materials feeding. This buffering device was used in Wugou Coal Mine, and the monitoring result shows that the maximum displacement of the buffering device is about 65 mm, which means this device is in a good operating condition.

1. Introduction

There are a lot of production materials that need to be transported from the surface to the underground everyday in coal mines. The materials required increased recent years with the development of fully mechanized solid backfilling mining because large amounts of solid materials [1–3], such as waste rocks, sand, stones, concrete, and other solid materials, are needed to be transported to the underground.

The traditional transport corridor for production materials in the coal mine is the main and auxiliary shafts. In order to save the transportation costs and increase the efficiency, however, a new transport technology was developed, which allows the solid materials to be directly transported from the surface to the underground through a vertical feeding shaft [4–6].

Fully mechanized solid backfilling coal mining is considered to be a safe and ecofriendly mining method and has been widely used in the coal seam under buildings, water bodies, and railways. In recent years, this new mining method has successfully mined five million tons of coal [7–9]. The solid backfill materials need to be continuously transported from the surface to the underground, which is key to increase the backfilling efficiency. Experiences have shown that a vertical feeding shaft provides the best path to transport solid materials [4, 10]. Because the mining depth of modern coal mines is large and the depth of vertical shaft may extend more than 1000 m, the falling speed of the solid backfill materials tends to be high, which causes the strong dynamic impact on the equipment at the bottom of the shaft. Therefore, a buffering device, which is installed at the bottom of the vertical feed shaft, is necessary to protect the lower part of the feeding shaft and the facilities in the materials storage bin. Among them, the stability of the buffering devices is especially important [11].

Many researchers have studied the vibration and dynamic responses of the buffering devices under the effects of impact loading in order to reveal influences on the stability of buffering devices. The common research methods include theoretical mechanics analyses, numerical simulation analyses, and laboratory experiments. Based on this, many researchers studied the dynamic mechanical responses of

buffering devices, in which the impact loading is caused by the aircraft landing gear [12], railway vehicle projects [13], and vehicle crash simulations [14]. The mechanisms associated with vertically falling discrete materials are complicated as a result of their high falling speed, which makes it difficult to study and design the suitable buffering devices.

In this paper, through theoretical analysis and numerical simulations, the dynamic mechanical relationship between the solid backfill materials and the impacted body was analyzed. And the mode and vibrational characteristics of each part of the buffering device were studied. Besides, the buffering mechanism of the vertically falling materials was discussed, which is of great significance for developing suitable buffering devices.

2. Solid Material Feeding System

The solid backfill materials can be efficiently transported with a solid material vertical feeding system. The process starts by performing screening, fragmentation, and other preprocessing activities on the solid backfill materials at the surface, and then those materials are transported through the feed shaft under rational control. Thus, the solid material vertical feeding system primarily consists of the ground processing, vertical feeding, and buffering systems, in which the vertical feeding system is mainly the feeding shaft and the buffering system is composed of the buffering device, as shown in Figure 1.

In order to minimize the kinetic energy of the solid backfill materials which fall to the bottom of the shaft, the buffering structure or device should be provided with the following features:

(1) A sufficient impact-resistant strength: the contact surface that is directly impacted by the solid backfill materials should be sufficiently strong to withstand the impacts resulting from the high falling speed of these materials.

(2) An energy storage mechanism: the solid backfill materials must be buffered, which means that the kinetic energy must be converted into other forms of energy that can be dissipated. Thus, during the high-speed collisions between the material and the buffering device, the buffering device should be provided with suitable structures that can convert the kinetic energy to other forms of energy and adapt to the impact displacement changes of the solid backfill materials. Therefore, the buffering device should have good elasticity.

(3) A stabilization framework: during the high-speed collisions between the solid backfill materials and the buffering device, the buffering device will experience significant vibrations. Therefore, there must be a stabilization framework that can support or lift the buffering device.

Based on the above analysis, a suitable buffering device should contain an impact-resistant contact body, energy storage system, and stabilization framework. The impact-resistant contact body uses a symmetrical structure, and the

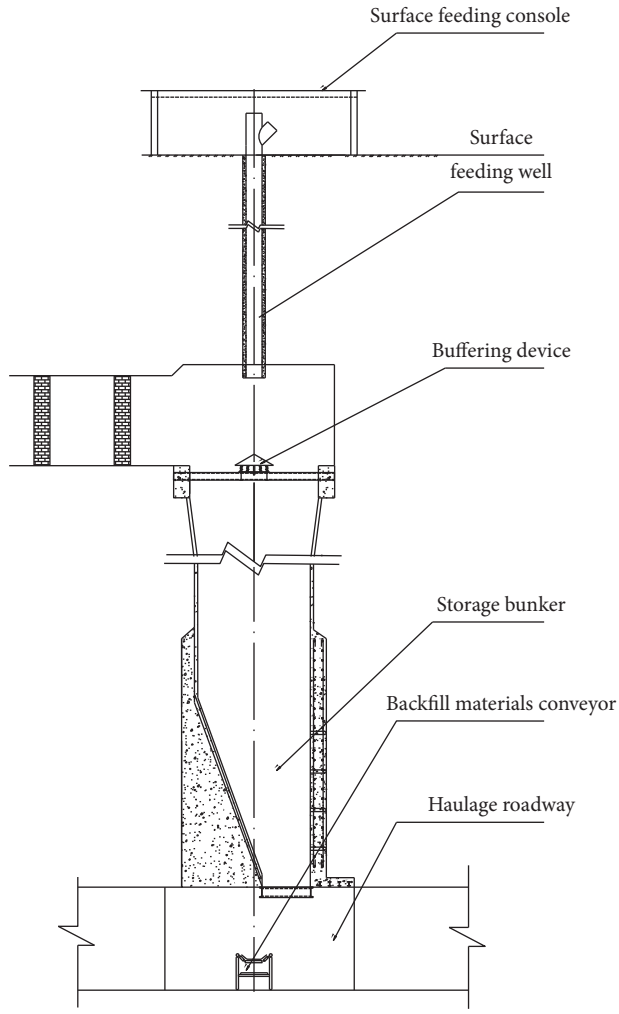

Figure 1: Solid filling material vertical feeding system.

structure of the collision contact surface is conical, in which the velocity of the solid backfill materials can be obviously changed. The energy storage system should have the capacity of coordinate deformation, and the structure is composed of two layers of circular elastic supporting seat and spring, which can be used to cushion the kinetic energy of the force and impact of the member. Because the suspension structure is relatively unstable during the collision process, the stabilization framework usually adopts the form of supporting beam, which can fix the buffer device on the surrounding structure. The impact-resistant contact body is fixedly connected with 1 guiding axis which passes through two holes of the center of the circular elastic supporting seat and is fixedly connected with the upper elastic supporting seat, and the lower elastic supporting seat is fixedly connected with the supporting beam. The buffering device is shown in Figure 2.

3. Mechanical Analysis on the Impact Process of Solid Filling Material in Vertical Delivery

3.1. Mechanical Model of Impact Process. According to the collision mechanical analysis characteristics of solid filling

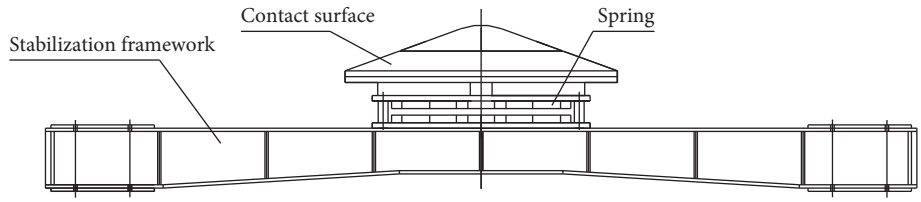

Figure 2: Diagram of the buffering device structure.

materials and buffering devices, some simplifications and assumptions be made to establish a collision mechanics model for solid filling materials and cushioning devices. First, the mechanical analysis only considers symmetric collision, and the collision is a single solid pair of cushioning devices and not considered a superposition of the dynamic load. Second, the analyzed solid backfill material is regarded as a sphere. Third, the friction of two objects is not considered when they collide. Fourth, the material rotation is not considered. Fifth, the difference in the size of the buffer spring deformation is not considered. A schematic diagram is shown in Figure 3.

3.2. Shock Displacement Equation. Through collision theory and rock dynamic characteristic [15, 16] test research, the collision between the solid backfill materials and the buffering device is divided into two cases, the elastic collision and the plastic collision.

3.2.1. Elastic Collision. The percussive force of the small ball and the buffer is P, and it is calculated according to Newton's second law of motion:

$$P = m_a \frac{dv_a}{dt} = -m_b \frac{dv_b}{dt}. \tag{1}$$

Deformation:

$$mP = \frac{d}{dt}\left(v_b - v_a\right) = \frac{d^2\delta}{dt^2},$$
$$m = -\frac{m_a + m_b}{m_a m_b}, \tag{2}$$

where m_a is the mass of the ball, m_b is the mass of the buffer device, v_a is the velocity of the ball, v_b is the velocity of the buffer device, and δ is the relative displacement of the small ball and the buffer device.

According to the Hertz theory, the relationship between P and static elasticity is static elastic relation (when the contact time is less than the stress wave time):

$$P = -\frac{4}{3} R^{1/2} E^* \delta^{3/2},$$
$$\frac{1}{E^*} = \frac{1 - v_a^2}{E_a} + \frac{1 - v_b^2}{E_b}, \tag{3}$$
$$\frac{1}{R} = \frac{1}{R_a} + \frac{1}{R_b},$$

where E^* is the synthetic elastic modulus of the small ball and the buffer device, E_a is the elastic modulus of the small ball, E_b is the elastic modulus of the buffer device, R is the synthetic radius of the small ball and the buffer device, R_a is the radius of the small ball, and R_b is the radius of the buffer device.

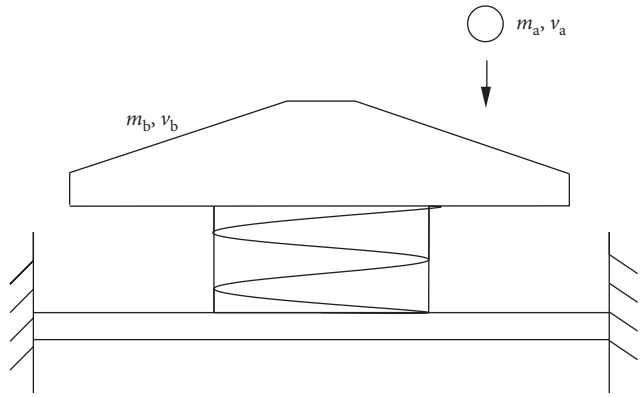

Figure 3: A schematic diagram of the collision process between solid filling material and buffer device.

According to the above, δ can be integrable:

$$\frac{1}{2}\left\{V_z^2 - \left(\frac{d\delta}{dt}\right)^2\right\} = \frac{3}{10}\frac{R^{1/2}E^*}{m}\delta^{5/2}, \tag{4}$$

where V_z is the speed of close proximity between the ball and the buffer device in initial moment.

When $d\delta/dt = 0$, the maximum compression of the ball and the buffer is δ^*, and the formula is as follows:

$$\delta^* = \left(\frac{15mV_z^2}{16R^{1/2}E^*}\right)^{5/2}. \tag{5}$$

When the spring under the buffer is impacted, according to Hooke's law, the formula for calculating the compression is as follows:

$$x = \frac{4R^{1/2}E^*\delta^{3/2}}{3K}, \tag{6}$$

where K is the stiffness of the spring.

Under the effect of concentrated load, the support beam meets the balance of the force in the vertical direction, and the simplified force is shown in Figure 4.

According to the structural mechanics, the deflection of the middle point of a supporting beam can be obtained:

$$\omega = \frac{13R^{1/2}E^*\delta^{3/2}l^3}{1875EI}. \tag{7}$$

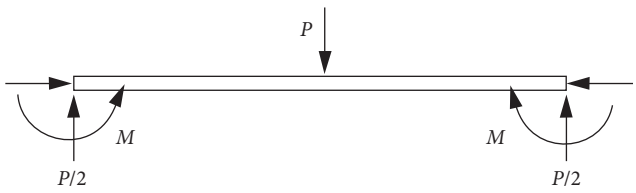

Figure 4: The force diagram of a supporting beam.

3.2.2. Plastic Collision. When the ball has plastic deformation due to the collision, according to the Tresca criterion, when the impact force is $p = 1.6Y$, the ball will yield deformation, where Y is the yield value of the unidirectional tensile ball, and the formula for calculating the yield force of the ball at Y point is obtained:

$$p_y^* = \frac{\pi^2 R^2}{6E^{*2}} P^2. \tag{8}$$

The force and deformation formulas of the elastic collision between the ball and the buffering device obtained in the elastic stage are substituted:

$$p_y^* = \frac{3}{2\pi}\left(\frac{4E^*}{3R^{3/4}}\right)^{4/5}\left(\frac{5mV_z^2}{4}\right)^{1/5}. \tag{9}$$

When the spring under the buffer is impacted, it is compressed; according to Hooke's law, the formula for calculating the compression quantity is as follows:

$$x = \frac{9\left(4E^*/3R^{3/4}\right)^{4/5}\left(5mV_z^2/4\right)^{1/5}}{8\pi R^{1/2}E^*}. \tag{10}$$

The yield force is used as the concentrated force of the beam and introduced into the deflection equation of the beam, and deflection of the middle point of the supporting beam can be obtained:

$$\omega = \frac{39l^3}{5000EI\pi}\left(\frac{4E^*}{3R^{3/4}}\right)^{4/5}\left(\frac{5mV_z^2}{4}\right)^{1/5}. \tag{11}$$

4. The Vibration Characteristics of the Buffering Device

4.1. Establishment of the Model. According to the structural model, the finite element model of the buffering device was established using the ANSYS software package. The buffering device is cone-shaped, and it is the main structure that consists of plates, beams, and springs. Models of the shells, beams, and springs are denoted as shell93, beam189, and combin14, respectively. 2 layers of circular elastic supporting seats are connected by 16 springs, which are evenly distributed in eight bearings. The supporting seat radius is 1000 mm, and the height of the spring is 200 mm. The double vibration beam with a stable structure adopts the structure of the hollow beam, the length is 6000 mm, the square section length is 500 mm, and the length of the hollow section is 300 mm. The ends of the lower beam are constrained to be fixed. All of the parts are attached to each other where they make contact. The protection cover and upper and lower bearing seats are separated by the shell units. The double reducing vibration beams are separated by the beam units.

In order to study the dynamic response during the collision process, the density of the plate and beam structure is set at 7800 kg/m^3, the modulus of elasticity is 210 GPa, and Poisson's ratio is 0.27. A spring-damper unit is used with a height of 200 mm, stiffness of 4.5×10^4 N/m, and zero mass. The completed finite element model is shown in Figure 5.

The working load of the buffering device depends on the falling speed of the solid backfill materials at the bottom of the feed shaft. During the falling process, which is very complicated, the solid backfill materials interact with the air. Systematic studies were carried out to better understand this interaction in the literature [11]. During a complete feed process, the feed volume first increases over time and then decreases. According to the law of motion for vertically falling solid materials [6], the loading caused by the solid materials on the buffering device can be simplified to a force that changes in the shape of a parabola, and it distributes in the central part of the diameter of 0.5 m. Equation (1) indicates the changes in the loading with different feed volumes:

$$F = -0.384t^2 + 7.76t, \tag{12}$$

where F represents the loading (kN) and t represents the time, and the value of t is from zero to 20 s.

4.2. Analysis of the Stress-Strain Result of the Buffering Device

4.2.1. Stress-Strain of the Contact Surface. When the feed process is underway, the buffering device experiences the impacts from the solid backfill materials, which results in stresses and strains on the contact surface. The strain value is negligible because of the high strength of the contact surface. At the instant when the impact occurs, the stress is concentrated on the contact surface. As time passes, the stress is dispersed over the circular plate that is used to support the lower spring. The Mises equivalent stress distribution as it changes over time is shown in Figure 6.

According to the Mises stress on the plate caused by the effects of the parabolic loading and the time-varying changes caused by the collisions, which are equal to the feed capacity, the distribution of the equivalent stress on the plate is petal shaped and increases to a maximum at the center before gradually decreasing toward the edge. Point A, which is 0.4 m distant from the plate center, and point B, which is 0.7 m distant from the plate center, were chosen in order to analyze the characteristics by which the stress on the plate spreads from the center to the edge. The Mises curve of the two points as they change over time is shown in Figures 7 and 8.

According to Figures 7 and 8, the Mises equivalent stress at each point on the plate is distributed over time in a parabolic way. At 10 s, when the feed capacity reaches its maximum, the stress on the plate also reaches its maximum. The vibration causes shaking at each point on the plate at a specific frequency because the lower part of the plate consists

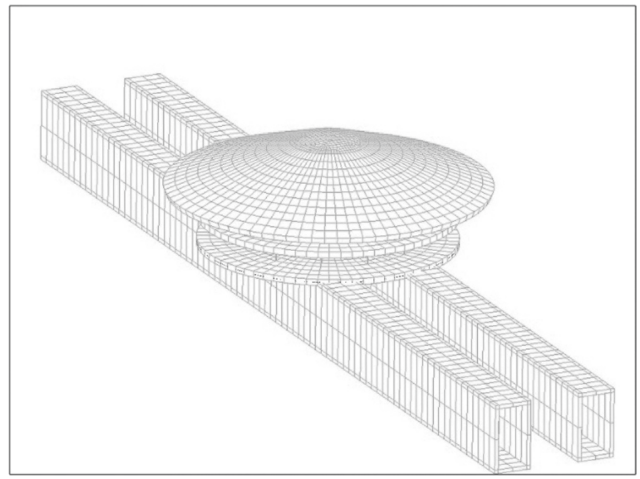

Figure 5: Finite element model of the buffering device.

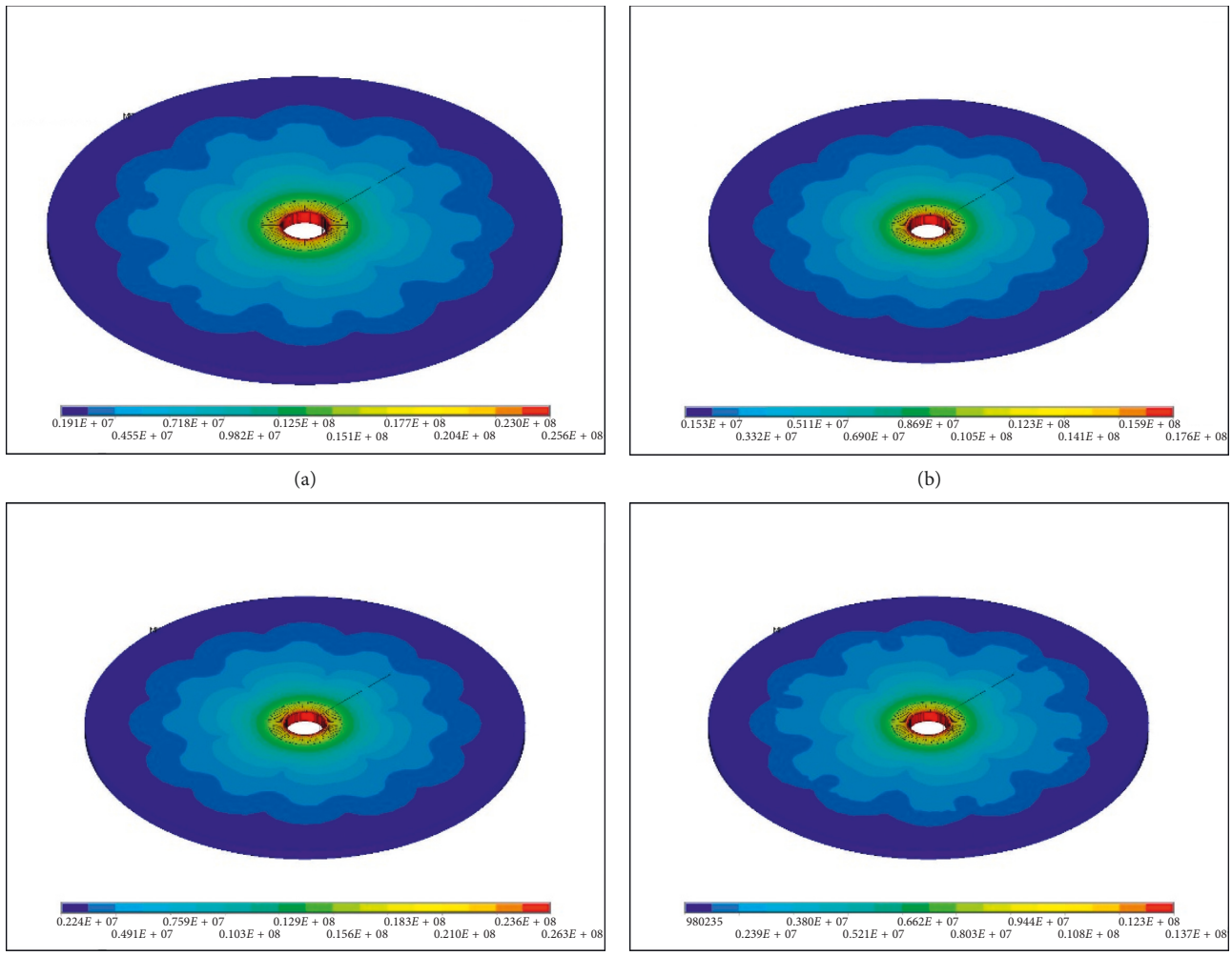

Figure 6: Mises stress distribution of the plate at different moments. (a) 1 s. (b) 5 s. (c) 10 s. (d) 20 s.

of spring units. Thus, the feed process of the solid backfill materials also exhibits an obvious shaking impact characteristic.

4.2.2. Vertical Displacement Changes in the Spring Units. In a buffering device, the spring units are important in terms of the actual buffering. The time-varying deformation curve

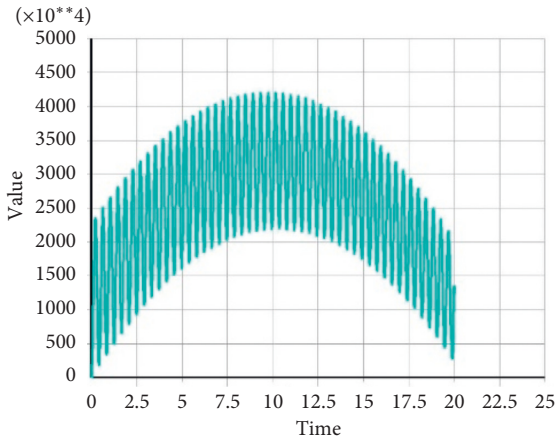

Figure 7: Mises equivalent stress curve of point A.

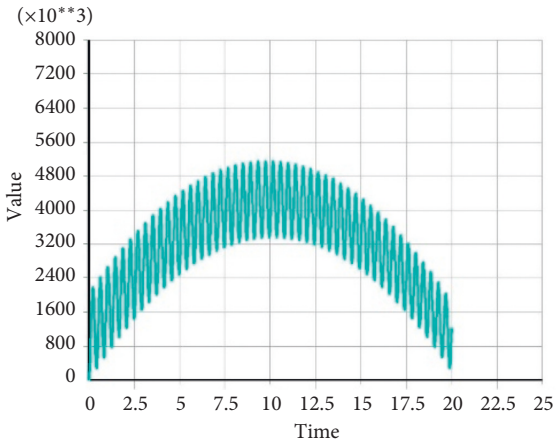

Figure 8: Mises equivalent stress curve of point B.

of the springs calculated by numerical modeling is shown in Figure 9.

According to Figure 9, the deformation of the springs changes over time and follows a parabolic characteristic. As the feed volume increases, the spring displacement exhibits an increasing vibration trend with a maximum displacement of approximately 90 mm.

4.2.3. Stress-Strain of the Support Beam. The cloud and bending moment diagrams of the Mises equivalent stress on the support beam calculated by numerical modeling when the feed of the solid backfill materials reaches its maximum are shown in Figure 10.

According to the above figure, with the effect of the periodic loading of the solid backfill materials, the stress on the support beam is highest at the ends and lowest at the center; the reason is that it has to do with the clamped ends of the support beam. With the effect of the periodic impact loading, there will eventually be impact damage on the ends of the support beam. Thus, when vertically feeding the solid backfill materials, the ends of the support beam are important. The method used to secure the support beam ends

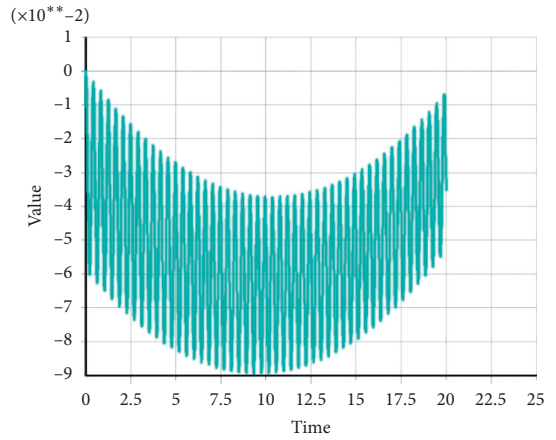

Figure 9: Time-varying deformation curve of springs.

in place is an important factor that should be accounted for when designing the buffering system.

5. Modal Analysis of the Buffering Devices

Modal analysis is a modern method designed to study the dynamic characteristics of structures and involves the application of system identification methods to the field of engineering vibration. The term "modal" refers to the intrinsic vibration characteristics of the mechanical structure. Every mode has a particular intrinsic frequency, damping ratio, and shape. The eighth-order mode of the buffering device obtained from the ANSYS analysis is shown in Figure 11. The intrinsic frequencies of the first- to eighth-order modes of the buffering device are shown in Table 1.

In order to better understand the stable forced vibration characteristics of the buffering device under changing loading conditions, we conducted a harmonic response analysis of the buffering device. In this case, the load was assumed to change sinusoidally because in practice during the feeding process, the load caused by solid materials impacting the buffering devices is distributed in a parabolic shape. The curve of the buffering device amplitude and phase angle, both of which change with frequency, is shown in Figures 12 and 13.

According to the buffering device amplitude-frequency and phase-frequency curves, when the frequency is at 2.4 Hz, the amplitude increases considerably and the degree change in the phase angle is approximately 90°, which means that resonance occurs in the structure at such a frequency. Compared with the previous modeling analysis, it is evident that this frequency is the intrinsic frequency (2.433 Hz) of the third order of the structure. This resonance pattern is characterized by an up-and-down vibration, which occurs in the upper structure of the buffering device springs. Care should be taken to avoid inducing this frequency when the structure is operating.

6. Case Study

6.1. Overview. The main mining seam of the Wugou Mine being operated by the Wanbei Coal-Electricity Group is #10

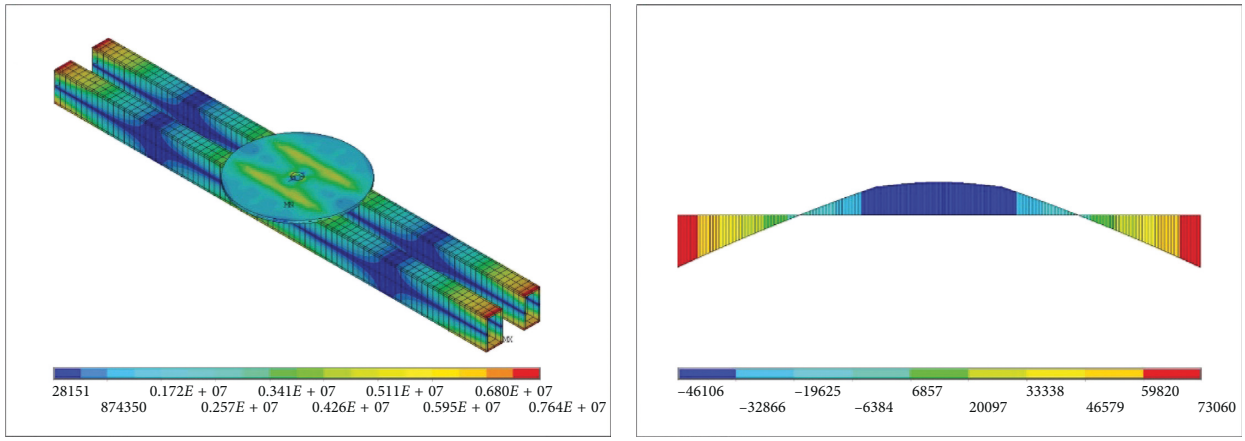

(a) (b)

Figure 10: Stress-strain characteristics of the support beam: (a) Mises equivalent stress contour; (b) bending moment diagram.

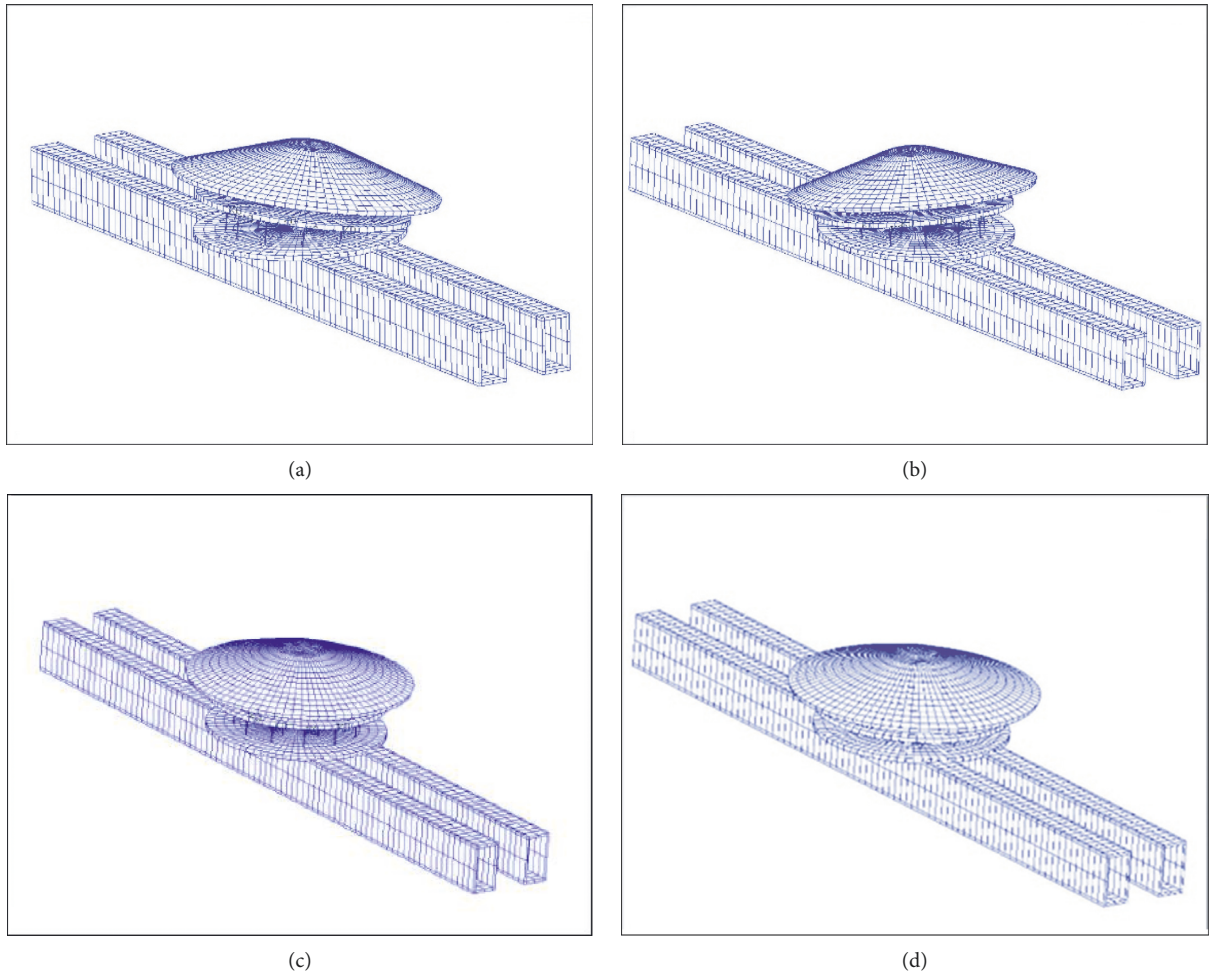

(a) (b)

(c) (d)

Figure 11: Continued.

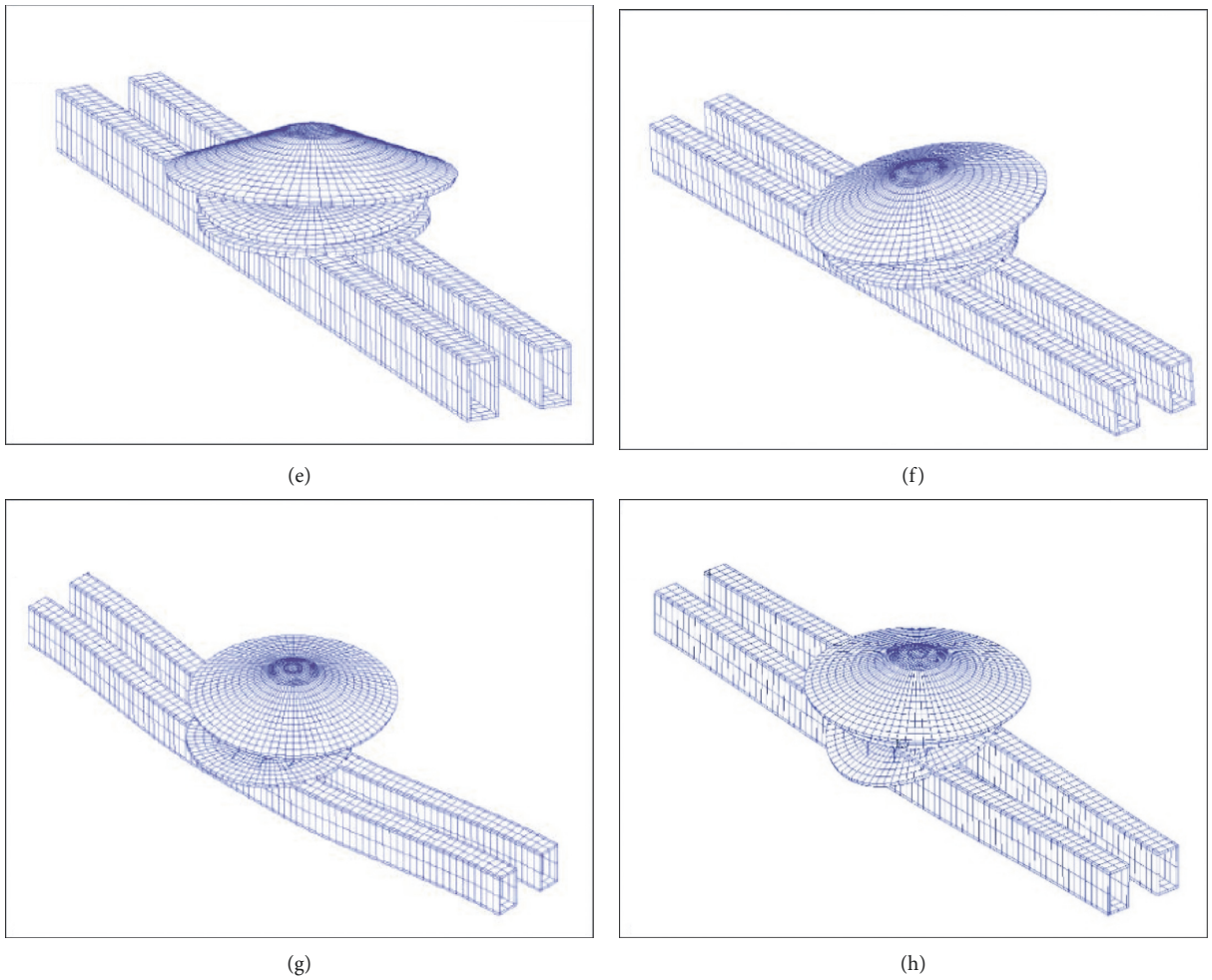

(e) (f) (g) (h)

Figure 11: Order mode of the buffering device: (a) first-order mode shape; (b) second-order mode shape; (c) third-order mode shape; (d) fourth-order mode shape; (e) fifth-order mode shape; (f) sixth-order mode shape; (g) seventh-order mode shape; (h) eighth-order mode shape.

Table 1: Order mode of the buffering device.

Order	Natural frequency (Hz)
1	1.3319
2	1.3351
3	2.4329
4	15.729
5	26.542
6	26.530
7	29.530
8	39.638

coal seam. A thick and loose aquifer that is approximately 272.9 m covers the coal seam, which poses a threat to coal mining safety. In order to improve the mining rate of the coal resources, fully mechanized solid backfill mining has been adopted. The fill materials used consist of gangues taken from the surface and are transported into the mine through the vertical feeding and transportation system. The diameter of the feed shaft is 50 mm, and the shaft is able to feed 550 t/h from the surface.

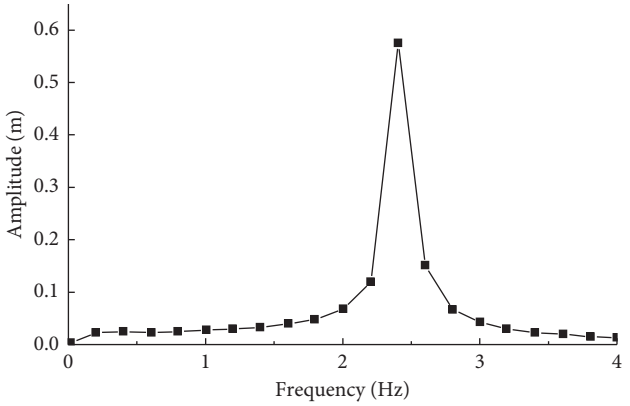

Figure 12: Buffering device amplitude-frequency curve.

Based on the above analysis, the designed buffering device consists of a protection cover, an energy storage shock absorber, and a double shock absorption arched beam. The protection cover, which was constructed using alloy materials with high strength and durability, is directly impacted by the solid backfill materials. The maximum diameter of the

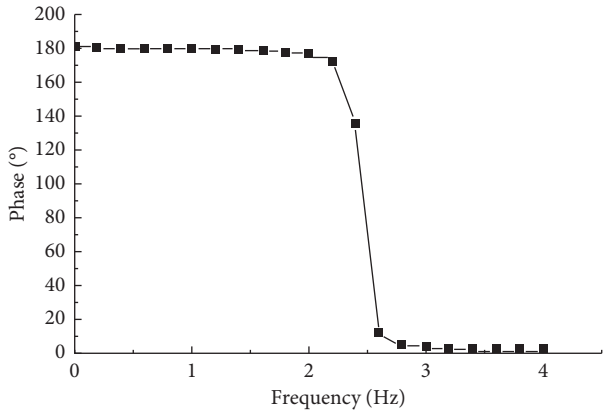

Figure 13: Buffering device phase-frequency curve.

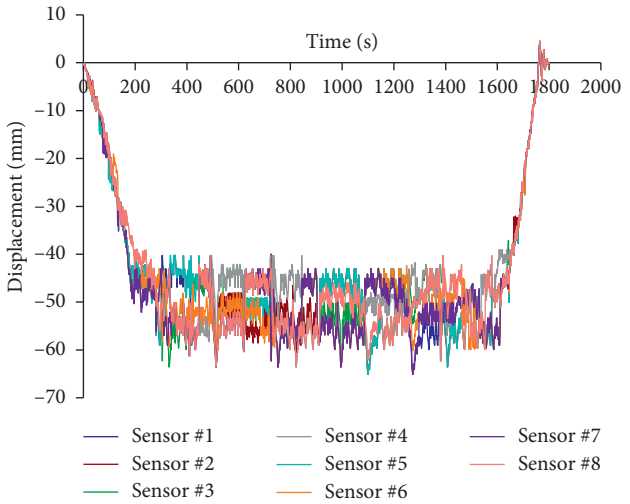

Figure 14: Time-varying change curve of buffering device displacement.

protection cover is 2.5 m. The energy storage shock absorber consists of 18 units of rubber springs with a height of 200 mm and stiffness of 4.5×10^4 N/m. The double shock absorption arched beam is a hollow square combination welded by 16Mn steel, and the length of the beam is approximately 7 m. The two ends of the beam, which are inserted into the storage bin wall, are poured with concrete, and the insertion depth is 500 mm.

6.2. Deformation Monitoring Analysis of the Buffering Device. Eight YWD-80 displacement sensors were installed in the vertical displacement space of the springs because the displacement of the cone-shaped buffering device mainly occurs on the springs of the energy storage shock absorber. The sensors were evenly attached to the outer springs of the buffering device. The TS832 multichannel program control dynamic strain indicator is used for data collection with a maximum frequency of 100 kHz. The sensors were placed into self-made spacing holes.

The system tested the deformation of the buffering device during the gangues feed process, and the test time is 30 minutes. The displacement curve of the buffering device as it changes over time is shown in Figure 14.

According to the figure, during the gangues feed process, the vertical displacement of the buffering springs on the cone-shaped buffering device gradually increased with the time-varying feeding. Within less than two minutes, the vertical displacement of the buffering springs reached their maximum, which was approximately 65 mm, although the vertical displacement value fluctuated above and below 50 mm. Within three minutes of the end of the feeding process, the vertical displacement value of the buffering springs gradually decreased before quickly returning to zero. When the stable feeding of solid materials occurred, the buffering device exhibited a dynamic characteristic in which fluctuations occurred around the maximum vertical displacement, which indicated that the buffering device operated as expected.

7. Conclusions

Based on the characteristics of the vertical feeding system, in this paper, the functional characteristics of the buffering devices have been analyzed by numerical simulation, and then the dynamic response and mode characteristics of these models were studied. In addition, a buffering device is designed. The conclusions are as follows.

Based on the analysis, three basic parts of the buffering structure were designed, including the impact-resistant contact body, energy storage system, and stabilization framework. A model consisting of the shell, plate, beam, and spring units was constructed using the ANSYS finite element numerical simulation software package. According to the simulation, as the feed capacity varies, the distribution of the equivalent stress on the buffering device plates was petal shaped, and the stress increased to a maximum at the center and gradually decreased toward the edge. The displacement of the spring changed in a parabolic way with a maximum value of approximately 90 mm. The stress on the support beam was highest at the ends and lowest at the center. With the effect of periodic impact loading, there will eventually be impact damage to the ends of the support beam.

By the method of theoretical analysis, based on the symmetrical collision condition of a single solid with a buffer, the elastic and plastic collision characteristics of a solid filling material and a buffer during a Hertz collision period were analyzed. The mechanical equation of the deflection of the buffer spring and the supporting beam was established.

A modeling analysis of the buffering device was conducted, and the intrinsic frequencies of the first to eighth orders of the structure were obtained. Through an analysis of the amplitude and phase angle of the structure, the frequency of resonance occurrence was calculated to be the intrinsic frequency (2.433 Hz) of the third order of the structure. It is believed that this resonance pattern corresponds to the up-and-down vibration which occurs in the upper structure of the buffering device springs. In general, this frequency should be avoided when the structure is operating.

Based on the basic characteristics of solid vertical feeding and the transportation system of the Wugou Mine, which is

under the Wanbei Coal-Electricity Group, a buffering device that consisted of a protection cover, an energy storage shock absorber, and a double shock absorption arched beam was designed. The testing results show that the maximum buffering device displacement is about 65 mm. The buffering device operates satisfactorily without incurring any damage.

Data Availability

The data used to support the findings of this study are included within the article.

Conflicts of Interest

The authors declare that there are no conflicts of interest regarding the publication of this paper.

Acknowledgments

The authors would like to thank the staff members in the Wugou Coal Mine for the help in the in situ test. The authors also thank the financial support from the National Natural Science Foundation of China (No. 51674241).

References

[1] X. X. Miao, J. X. Zhang, and G. L. Guo, "Study on waste-filling method and technology in fully-mechanized coal mining," *Journal of China Coal Society*, vol. 35, no. 1, pp. 1–6, 2010.

[2] H. Pu and J. Zhang, "Research on protecting the safety of buildings by using backfill mining with solid," *Procedia Environmental Sciences*, vol. 12, pp. 191–198, 2012.

[3] Z. F. Bian, X. X. Miao, and S. G. Lei, "The challenges of reusing mining and mineral-processing wastes," *Science*, vol. 373, no. 6095, pp. 701–703, 2012.

[4] F. Ju, J. Zhang, and Q. Zhang, "Vertical transportation system of solid material for backfilling coal mining technology," *International Journal of Mining Science and Technology*, vol. 22, no. 1, pp. 41–45, 2012.

[5] N. Zhou, Q. Zhang, F. Ju, and S. W. Liu, "Pre-treatment research in solid backfill material in fully mechanized backfilling coal mining technology," *Disaster Advances*, vol. 6, pp. 118–125, 2013.

[6] F. Ju, B. Y. Li, and S. Guo, "Dynamic characteristics of gangues during vertical feeding in solid backfill mining: a case study of the Wugou coal mine in China," *Environmental Earth Sciences*, vol. 75, no. 20, 2016.

[7] B. S. Hao, "Technology of full- mechanized stowing mining under buildings," *Coal Mining Technology*, vol. 15, pp. 39–41, 2010.

[8] P. Gong, Z. G. Ma, X. Y. Ni, and R. R. Zhang, "Floor heave mechanism of gob-side entry retaining with fully-mechanized backfilling mining," *Energies*, vol. 10, no. 12, p. 2085, 2017.

[9] J. Zhang, B. Li, N. Zhou, and Q. Zhang, "Application of solid backfilling to reduce hard-roof caving and longwall coal face burst potential," *International Journal of Rock Mechanics and Mining Sciences*, vol. 88, pp. 197–205, 2016.

[10] F. Ju, *Development and engineering applications of solid materials vertical transportation system in backfill coal mining technology*, PhD Thesis, China University of Mining and Technology, Xuzhou, China, 2012.

[11] J. X. Zhang, B. F. An, and F. Ju, "Influence factors of solid material particles motion in the feeding system of fully mechanized coal mining and backfilling," *Journal of Mining and Safety Engineering*, vol. 29, no. 3, pp. 312–316, 2012.

[12] F. Zhang, X. F. Yan, and Y. S. Liu, "Reliability parameter sensitivity analysis for aircraft landing gear shock absorber," *Journal of Vibration Engineering*, vol. 28, no. 1, pp. 67–72, 2015.

[13] R. Tekade, C. Lingua, and C. Patil, "Structural and modal analysis of shock absorber of vehicle," *International Journal of Engineering Trends and Technology*, vol. 21, no. 4, pp. 173–186, 2015.

[14] N. Frisch, D. Rose, O. Sommer, and T. Ertl, "Visualization and pre-processing of independent finite-element meshes for car crash simulations," *Visual Computer*, vol. 18, no. 4, pp. 236–249, 2014.

[15] F. Q. Gong, X. B. Li, and X. L. Liu, "Experimental study on rock mechanical properties under combined 3-D static and dynamic loading," *Chinese Journal of Rock Mechanics and Engineering*, vol. 30, no. 6, pp. 1179–1190, 2011.

[16] X. B. Li, F. Q. Gong, K. Gao, and T. B. Yin, "Experimental study on rock impact failure under combined one-dimensional static and dynamic loading," *Chinese Journal of Rock Mechanics and Engineering*, vol. 2, pp. 251–260, 2010.